Proceedings of the 30th International Cosmic Ray Conference
Rogelio Caballero, Juan Carlos D'Olivo, Gustavo Medina-Tanco,
Lukas Nellen, Federico A. Sánchez, José F. Valdés-Galicia (eds.)
Universidad Nacional Autónoma de México,
Mexico City, Mexico, 2008

Vol. 5 (HE part 2), pages 1401–1404

30TH INTERNATIONAL COSMIC RAY CONFERENCE

Search for Supernova Relic Neutrino at Super-Kamiokande

TAKASHI IIDA[1]
FOR SUPER-KAMIOKANDE COLLABORATION
[1]*Kamioka Obserbatory, ICRR, University of Tokyo, Higashi-Mozumi, Kamioka*
iida@suketto.icrr.u-tokyo.ac.jp

Abstract: Supernova relic neutrinos (SRN) is diffuse supernova neutrino background from all past supernova. No experiments has succeeded in detecting SRN yet. In this paper a search for SRN was conducted using Super-Kamiokande (SK) data. SK is a large water Cherenkov detecter in Kamioka, Japan. In this analysis, 791 days' data taken in the second phase of SK (SK-II) was used and $\bar{\nu_e}$ signals in the neutrino energy range above 19.3MeV were searched. The observed spectrum is consistent with the expected background spectrum and a flux upper limit of 3.68 /cm^2 /sec was obtained with 90 % confidence level. A similar search using SK-I data gave a flux upper limit of $<$1.25 /cm^2 /sec. By the combined analysis of SK-I and SK-II, a flux upper limit of $<$ 1.08 /cm^2/sec was obtained.

Introduction

In 1987, Kamiokande detected neutrinos originating from SN1987A, a core colapse supernova that occured in The Large Magellanic Clouds[1]. It proved that this type of supernova emit an energy about 10^{53} ergs in the form of neutrinos. Since the beginning of universe, innumberable supernovae have occured. Neutrinos from such supernovae should be observable now as a diffused background all over the universe; this is known as Supernova Relic Neutrino (SRN). SRN is a very interesting observational target in astrophysics. Measurement of SRN will enable us to investigate the history of past supernova. For example, the flux of SRN would indicate the star formation rate and supernova rate in galaxies. Although underground experiments in the last decade searched for SRN, none of them have observed SRN signal yet. There are several models[3-8] which predict the SRN flux and spectrum. As it will be described later, the flux upper limit of SK is getting close to the prediction.

We searched for SRN using Super-Kamiokande(SK), a large water Cherenkov detector located at Kamioka mine in Japan. SK is a high-performance neutrino detector consisting of 11,146 20-inch PMTs and 50,000 tons of pure water. The fiducial mass for this search is 22.5 kton, which is defined to be more than 2m from the walls of the detector. SRN includes all six types of neutrinos, but the main interaction for the SRN search in the SK detector is the charged current quasi-elastic interaction of inverse β decay($\bar{\nu_e}$ + p $\rightarrow$ e^+ + n). SK has collected data in three phases so far. The first phase (SK-I) is from April 1996,the begining of SK, to July 2001. The second phase (SK-II) was started from December 2003 and finished in October 2005. In SK-II, the number of PMTs is about half of SK-I. The third phase of SK (SK-III) was started in July 2006 after the number of PMTs were recovered to the same as SK-I. A search for SRN using SK-I data is reported in [2] and a flux upper limit of $<$1.2 /cm^2/sec was obtained. In this report, a search for SRN using SK-II data is described.

Data reduction

In this analysis, 791 days' data of SK-II taken from December 2003 to October 2005 is used. The backgrounds to the SRN search are solar neutrinos, atmospheric neutrinos, and muon-induced spallation products. In order to minimize the contribution of those backgrounds, the energy range adopted in this analysis is between 18 MeV and 82 MeV in visible energy (i.e. total energy of

positron in the detector). The energy of positron is $E_{\bar{\nu_e}} - 1.3MeV$.

Background reduction was applied to data in the following steps:

- Normal spallation cut

  Cosmic ray muons can spall oxygen and induce unstable nuclei called spallation products (μ + $^{16}O \rightarrow \mu$ + X). It is one of the most abundant background in this energy region, and the ability to remove the background determines the lower threshold of the SRN search. The spallation background is reduced by a likelihood method that uses timing and track information of the muons preceeding the candidate events. This cut algorithm is the same as the one used in the solar neutrino analysis of SK.

- Cherenkov angle cut,

  The remaining muons are removed by a Cherenkov angle cut. The source of muons is from the interaction of atmospheric muon neutrinos. Positrons with E$>$ 18 MeV have a Cherenkov angle of $\theta_C \sim$ 42 degrees. Muons that still remain in the SRN search have p$_\mu <$ 350MeV, which corresponds to $\theta_C <$ 38 degrees; thus, the events with $\theta_C <$ 38 degrees were removed from the data. The Cherenkov angle cut is also used to remove events with $\theta_C >$ 50 degrees; this eliminats events without a clear Cherenkov ring pattern, such as multiple γ rays emitted by a nuclear de-excitation.

- Solar direction cut

  In order to remove solar ν events, the events in the direction of the sun are removed. Solar ^{8}B and hep ν_e's are detected in SK as recoil electrons from elastic scattering. Direction θ_{sun} is defined as the angle between the recoil direction and the Sun's direction. Events have lower energy ($<$25MeV) and small θ_{sun} ($cos\theta_{sun} >$ 0.75) are rejected.

- Tight spallation cut

  In addition to the normal spallation cut, tighter criteria is applied in order to enhance the rejection efficiency of spallation background. Higher energy beta ray products usually have shorter lifetime. So, we remove events which occure within 0.15 sec from cosmic ray muons.

- Sub-event cut

  Charged current interactions of atmospheric ν_μ produce muons and decay electrons. Some decay electrons survive in this analysis but are tagged by preceeding muons. Some fraction of those muons may have past Cherenkov angle cut but are identified by the following decay electron. In order to remove those backgrounds we remove the events which has time correlating events before or after the candidate events. By careful reevaluation of SK-I data number of events is reduced from 271(SK-I published data) to 218 events.

- Gamma ray cut

  Some events originating from outside of the fiducial volume have the possibility of being reconstructed within the fiducial volume of SK. γ-rays from the materials of the detector structure and surrounding rock is the source of these backgrounds. We remove the events expected travel distance of γ rays through the detector(the distance projected backwards from vertex) is less than 450cm.

Analysis and Results

The number of events remaining in each reduction step is listed in Table 1.1 and the spectrum is shown in Figure 1. After all cuts are apllied, 115 SRN candidates remain. Most these candidates are due to three kinds of irreducible backgrounds.

Reduction step	Remaining event
Normal spallation cut	569
Cherenkov angle cut	241
Solar direction cut	228
Tight spallation cut	213
Sub-event cut	123
Gamma ray cut	115

Table 1: The number of events remaining at each reduction step in SK-II is listed.

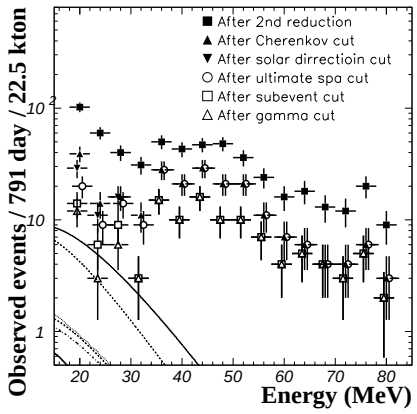

Figure 1: Spectrum of data at each reduction step. Lines represent theoretical predictions

The first background is spallation events from cosmic ray muons which still remain past the two spallation cuts descrived above. We estimate the number of remaining spallation background using the quality of rejected spallation events. The estimated number of background is 8.2 events/791days in 18-22MeV.

Other two backgrounds are ν_e and ν_μ components of atmospheric neutrinos. ν_e component means atmospheric ν_e and $\bar{\nu}_e$ which correspods to the red-dotted histogram in Figure 2. ν_μ component is atmospheric ν_μ and $\bar{\nu}_\mu$ which produce muons below Cherenkov threshold and decay electrons observed in the detector(invisible muon) The spectrum of 'invisible muon' is a Michel spectrum as shown by the green-dotted histgram in Figure 2. The spectrum shape of these two backgrounds are obtained by atmospheric MC simulation.

The energy spectrum of these backgrounds have shapes that are very different from each other and from the SRN signal shape. Data are divided into sixteen energy bins and the following χ^2 function is minimized with respect to α, β and γ. The flux of SRN is obtained by fitting the observed spectrum with a mixture of those background spectra.

$$\chi^2 = \sum_{i=1}^{16} \frac{(N_{Data}(i) - N_{Spec}(i))}{\sigma^2} \qquad (1)$$

$$N_{Spec}(i) = \alpha \times N_{SRN}(i) + \beta \times N_{atm\nu_e}(i) + \gamma \times N_{atm\nu_\mu}(i) + N_{Spal}(i)$$

Where the sum is over all energy bins and N_{data}(i) is the number of events in i^{th} bin. N_{SRN},$N_{atm\nu_e}$,$N_{atm\nu_\mu}$,N_{Spal} are the number of events in i^{th} bin for expected SRN signal, atmospheric ν_e component, atmospheric ν_μ component, and the estimated spallation background, respectively. α, β, and γ are the normalization factor of each component and are tuned to minimized χ^2.

The spallation factor is constant 1 because the number of spallation events are already estimated. Figure 2 shows the fitting result: the black histogram is best fit background and signal spectrum. For all six models, the best fit to α is 0 and minimum χ^2 is 10.4 for 13 d.o.f. Thus, 90 % C.L. α limit is set to each model and 90% SRN flux upper limit is derived using the α limit.

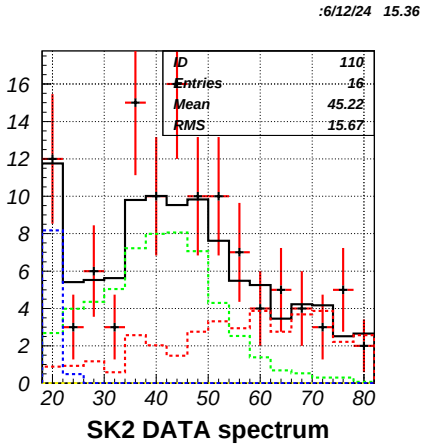

Figure 2: Energy spectrum of data and fitted background spectrum. Blue-dotted histgram (which has peak in the first bin) is remaining spallation background and green-dotted histgram(peaked at around 40MeV) is atmospheric ν_μ. Red-dotted histogram is corresponding to ν_e. Solid histgram is thair sum.

The SRN limit depends on the shape of the theoretical spectrum. But it is not so sensitive in our analysis region (E_ν >19.3MeV) because the spectrum shape of all models are very similar in each other in this energy region. Thus the obtained flux

limit for six models are almost the same value: $\sim$ 3.7 /cm^2/sec.

A similar analysis was applied to SK-I data and a flux upper limit of < 1.25/cm^2/sec was obtained. It is slightly different from the value published in [2], because (1) sub-event cut was improved by careful inspection of neighboring events, and (2) cross section of the inverse beta decay was revised from 0th ordered approximate cross section to higher ordered one [9].

Finally SK-I and SK-II analysis are combined using following method. Figure 3 shows χ^2 and probabirity (calculated using χ^2) distribution as a function of flux normalizing facor α. The red lines and green lines correspond to SK-I and SK-II respectively. Combined χ^2 are the blue lines. The combined 90% flux limit is obtained as 1.08 $/cm^2/sec$. Figure 4 shows the SK-I, SK-II and combined flux limit and theoretical flux prediction of SRN for each model.

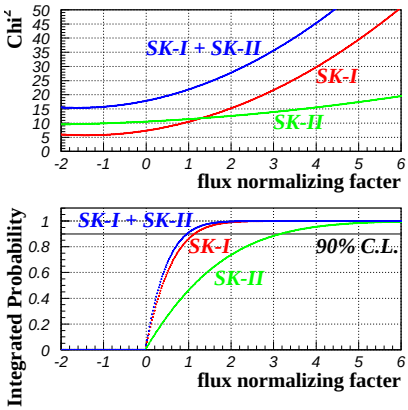

Figure 3: χ^2 and probability as a function of flux normalizing factor α

Conclusion

A search for SRN is conducted at Super-Kamiokande to detect the diffuse $\bar{\nu}_e$ signal. Although 115 candidate events remain after a reduction for the 791days' SK-II data, the spectrum is consistent with the background and excess of signal was not found in this analyis. Using six kinds

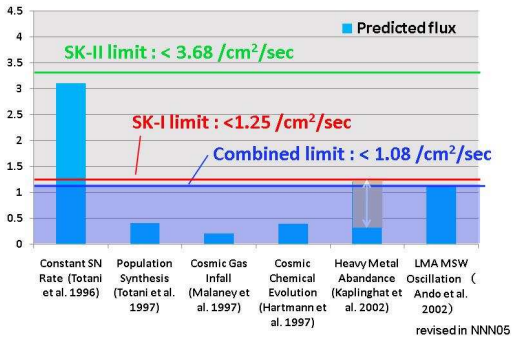

Figure 4: SRN flux limit in SK and model predicted flux.

of SRN models, 90% C.L. SRN flux limit is obtained to be < 3.68 /cm^2/sec.

This SK-II limit is worse by a factor three compared to that from SK-I,$<$ 1.25 /cm^2/sec, due to SK-II's reduced livetime and energy resolution. The combined analysis of SK-I and SK-II yields a flux limit of 1.08 cm^2/sec. This is the world's most stringent limit on the SRN flux.

References

[1] K.S. Hirata et al. Phys. Rev. Lett. **58**, 1490 (1987).

[2] M. Malek et al. Phys. Rev. Lett 90, 061101 (2003)

[3] T. Totani and K. Sato, Astropart. Phys. **3**, 367 (1995).

[4] T. Totani, K. Sato, and Y. Yoshii, Astrophys. J. **460**, 303 (1996).

[5] R. A. Malaney, Astropart. Phys. **7**, 125 (1997).

[6] D. H. Hartmann and S.E. Woosley, Astropart. Phys. **7**, 137 (1997).

[7] M. Kaplinghat, G. Steigman, and T. P. Walker, Phys. Rev. D **62**, 043001 (2000).

[8] S. Ando, K. Sato, and T. Totani, Astropart. Phys. **18**, 307 (2003).

[9] A. Strumia and F. Vissani Phys. Lett. B564 42-54 (2003).